Fault growth and acoustic emissions in confined granite

David A Lockner and James D Byerlee

U.S. Geological Survey, 345 Middlefield Road, Menlo Park, CA 94025

The failure process in a brittle granite was studied by using acoustic emission techniques to obtain three dimensional locations of the microfracturing events. During a creep experiment the nucleation of faulting coincided with the onset of tertiary creep, but the development of the fault could not be followed because the failure occurred catastrophically. A technique has been developed that enables the failure process to be stabilized by controlling the axial stress to maintain a constant acoustic emission rate. As a result the post-failure stress-strain curve has been followed quasi-statically, extending to hours the fault growth process that normally would occur violently in a fraction of a second. The results from the rate-controlled experiments show that the fault plane nucleated at a point on the sample surface after the stress-strain curve reached its peak. Before nucleation, the microcrack growth was distributed throughout the sample. The fault plane then grew outward from the nucleation site and was accompanied by a gradual drop in stress. Acoustic emission locations showed that the fault propagated as a fracture front (process zone) with dimensions of 1 to 3 cm. As the fracture front passed by a given fixed point on the fault plane, the subsequent acoustic emission would drop. When growth was allowed to progress until the fault bisected the sample, the stress dropped to the frictional strength. These observations are in accord with the behavior predicted by Rudnicki and Rice's bifurcation analysis but conflict with experiments used to infer that shear localization would occur in brittle rock while the material is still hardening.

INTRODUCTION

Significant effort has been made in recent years in the study of the processes controlling crack propagation in brittle materials. Recent laboratory studies of rocks have been devoted primarily to the measurement of physical properties (fracture toughness K_I, subcritical crack growth rates, etc.) for mode I crack growth in pure tension [*Atkinson and Meredith*, 1987]. Experimental apparati such as the Double Cantilever Beam assembly have been refined so that parameters such as K_I and crack growth rate can be accurately determined. Since the overall stress state at earthquake hypocentral depths is compressive, large scale crustal failure is inherently a shear faulting phenomena and can only involve tensile crack growth on the microscopic scale. Because of the importance of understanding earthquake processes, considerable laboratory effort has been devoted to the study of rock failure in compression. Much of this effort has been devoted to the study of precursory changes leading up to fault formation and failure. However, because faulting in brittle rock tends to occur unstably, direct laboratory measurements of the growth of shear fractures have been limited. *Rice* [1980], *Wong* [1982] and *Lockner et al.* [1991], for example, have analyzed the energy dissipation during fracture in compression to estimate shear fracture energy release rate G. We have recently employed a new technique to stabilize the growth process of a macroscopic fault in a brittle rock [*Lockner et al.*, 1991a, b]. This has allowed us to observe, for the first time, the complete nucleation and growth phases of a shear fracture. In addition, source locations of acoustic emission (AE) events were determined from acoustic travel time data. Through these techniques, we have been able both to confirm long-standing ideas and to gain new insight into the process of brittle faulting.

EXPERIMENTAL PROCEDURE

Confined, triaxial deformation experiments have been conducted on intact samples of Westerly granite. All samples were precision ground to a length of 19.05 cm and a diameter of 7.62 cm. Each sample was jacketed in a polyurethane tube or thin-walled Cu tube with six

piezoelectric transducers (resonance at 0.6 MHz) attached to the rock surface to monitor stress-induced AE signals (Fig 1). In most experiments, a set of four additional transducers periodically measured the P-wave velocity field to aid in the hypocentral inversion routine. All samples were deformed at constant confining pressure P_c = 50.0 ± 0.2 MPa. One granite sample was deformed in creep, at a constant differential stress ($\sigma_c = \sigma_1 - P_c$) of 510 MPa. Described in more detail in *Lockner and Byerlee* [1980], this sample failed violently after 2.5 days. To analyze the details of the rapid faulting process, an attempt was made to stabilize the violent break-down phase of the fault formation. Stabilization was accomplished by attaching a fast-acting hydraulic valve to the ram that controlled axial load. By adjusting σ_1 to maintain approximately constant AE rate, the rapid strength loss associated with fault formation was successfully anticipated and slowed to where it occurred over a period of minutes to hours. Furthermore, by limiting the overall AE rate, we could be assured that the AE acquisition system would never become saturated (a design constraint of 300 events per second), so that we were able to record the complete sequence of microcrack events. In this way we avoided what may be a significant sampling problem present in many of the AE rock failure studies in the literature. Axial displacement was measured outside the pressure vessel while circumferential strain was measured with a foil strain gage attached to the mid-plane of the sample. This procedure and the hypocentral location scheme are described in more detail in *Lockner et al.* [1991b].

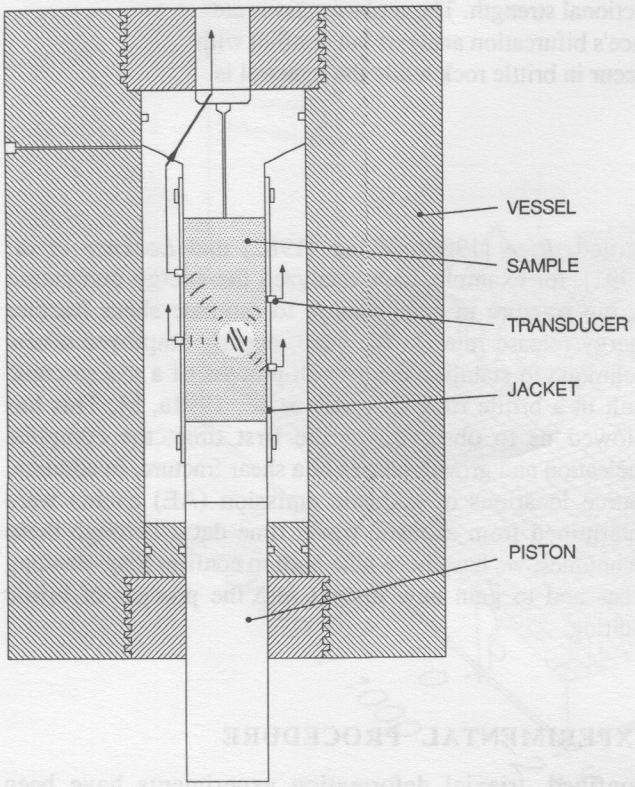

FIG 1. Schematic view of sample mounted in pressure vessel. Six piezoelectric transducers mounted on sample surface detected acoustic emissions during deformation. An additional set of four transducers was used to determine velocity field.

Measurement precisions for σ_1 and P_c were nominally ±0.2 MPa. Axial displacement precision was $\pm 0.03 \times 10^{-3}$ cm. Strain gage sensitivity was $\pm 1 \times 10^{-6}$ for short time intervals but was degraded by thermal drift to a long-term stability of $\pm 5 \times 10^{-6}$. Of greater importance for the results presented in this paper are the hypocentral location accuracies for the AE events recorded in these experiments. Since an automatic threshold detector is used in the acquisition system, there is a tendency to pick small-amplitude arrivals too late. Such timing errors will result in large travel time residuals in the inversion routine and can therefore be recognized. For larger amplitude events that give rms travel time errors ≤ 1μs, location precision is ±0.3 cm. Piezoelectric transducers are mounted on the sample surface to provide excellent sensor coverage for events occurring in the central region. Coverage is not as good near the ends of the sample and absolute location accuracy decreases in these regions. Even so, relative accuracy of neighboring events, which is important in discussing the present results, remains good near the sample ends. This is demonstrated by the tight clustering of events on the propagating fault plane (*e.g.* Figs 5 and 6).

USE OF ACOUSTIC EMISSION TO STUDY FAULT DEVELOPMENT

Fracture experiments employing AE location techniques typically fall into three categories. In the first case, cyclic loading experiments have been conducted (*e.g. Sondergeld and Estey*, 1981), in which axial stress is cycled until sample failure. In these experiments, the microcrack damage that accumulates during each cycle is analyzed for progressive clustering or migration of event locations. A second type of experiment involves deformation of the sample at constant strain rate (*e.g. Weeks et al.*, 1978), with axial stress acting as a dependent variable. This is more like the natural case where one might consider a crustal fault being loaded remotely due to deformation of the mantle. However, since laboratory strain rates (typically greater than 10^{-7} s^{-1}) are orders of magnitude greater than crustal rates, important time-dependent processes such as subcritical crack growth may not be given adequate time to occur on the laboratory scale. The third common deformation experiment (*e.g. Lockner and Byerlee*, 1980; *Nishizawa et al.*, 1984; *Yanagidani et al.*, 1985; *Hirata et al.*, 1987), known as a

creep test, is conducted at a constant, pre-determined stress level (generally between 70 and 90% of the short-term failure strength). Since stresses would not be expected to vary significantly in the hours or days preceding an earthquake, a creep test may provide a good analog for the natural situation applicable to short-term precursors. However, a significant drawback to the use of creep tests to study fracture is the inherent unbounded increase in AE activity and strain rate that accompanies fault nucleation.

Fault nucleation in creep test

Despite the inherent limitations in using creep tests to study fault propagation, useful information can be obtained related to the pre-nucleation and nucleation stages of fault formation. As an example of this, we show AE hypocentral locations from a creep test on Westerly granite in Fig 2. Events have been plotted in four time intervals to show the change in microcracking over the course of the experiment. During primary and secondary creep (first two plots), AE events are distributed broadly throughout the central region of the sample. A general feature of these experiments is that AE activity is reduced near the ends of the sample due to contact with the rigid steel end plugs which inhibit dilatancy and the associated microcrack damage in the adjacent rock. The onset of tertiary creep (third plot) coincides with the sudden appearance of a concentrated nucleus of microcracking on what is to become the fault plane. This nucleation zone is approximately 1.5 cm in diameter and shows a tendency to be oriented along the direction of the fault. In the last 18 minutes before failure (fourth plot, Fig 2), the nucleation zone has extended itself along the direction of the eventual fault. Since the loading system attempts to maintain constant stress in a creep experiment, the final stage of fault growth is an inherently unstable process. As a result, less than one-third of the total fault plane growth could be monitored in this experiment before unstable propagation ended the experiment.

The diffuse AE activity during primary and secondary creep indicates that in these early stages of deformation, microcracking is essentially self-hardening: individual microcrack events relieve local stress concentrations and redistribute stresses more uniformly over larger regions. Westerly granite has been chosen for its small grain size and uniformity. By contrast, other materials, with large pre-existing flaws, would be expected to show localized AE activity from early in the loading cycle. Sandstone

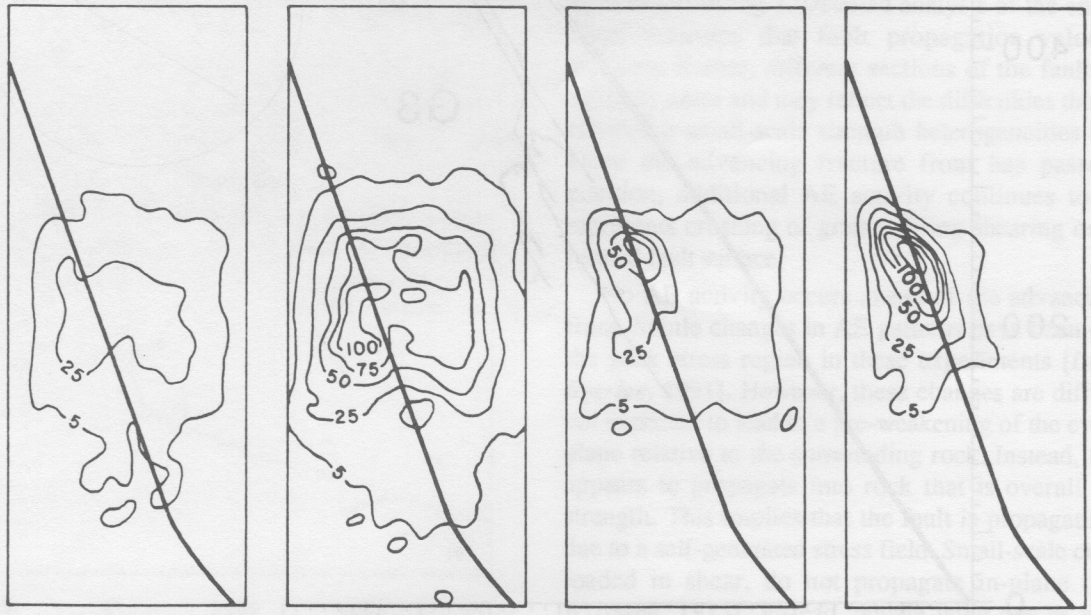

FIG 2. Plot of density of acoustic emission source locations for initially intact sample of Westerly granite [from *Lockner and Byerlee,* 1980]. a) Primary creep; b) secondary creep; c) initial 133 minutes of tertiary creep and d) final 18 minutes of tertiary creep. In all plots, the sample is viewed along-strike of the eventual fracture plane (shown for reference as a diagonal line). Rather than plotting individual events, contours are constructed that show the density of events per cm^2 in each projection.

experiments, described in *Lockner et al.* [1991b] provide good examples of the effects of larger-scale pre-existing flaws. In a related point, we found that no obvious change in the AE pattern was observed between primary and secondary creep in the granite experiment, suggesting that secondary creep may not be the result of a unique process.

In contrast with the uniform microcracking observed in the early stages of creep, tertiary creep was clearly associated with fault nucleation, and represents a fundamental shift in the mode of microcracking. The appearance of the nucleation cluster was quite abrupt. After 58 hr of diffuse activity, the cluster of events marking the onset of tertiary creep occurred in minutes. While this sudden increase in activity indicates a local loss of strength, the sample, as a whole, was still able to support the average stress applied by the loading system. This response shows how mechanical instability is due to an interaction of the loading system and the fault. The accelerating creep leading into unstable fault propagation has a direct parallel in mode I crack growth. In this case, cracks will extend at slow rates when $K_I < K_{IC}$ (subcritical crack growth) and grow unstably when $K_I = K_{IC}$.

Quasi-static fault growth

In the creep experiment described in the preceding section, we demonstrated that accelerating tertiary creep marked the transition from distributed microcrack damage to organized and clustered damage along what was to become the macroscopic fault plane. However, the late stages of fault propagation could not be observed since fault growth was too rapid. A constant AE rate feedback system was therefore developed to stabilize the faulting process and allow for a more detailed observation of the propagation phase. Stress/displacement and stress/time curves for two granite samples deformed at 50 MPa confining pressure are shown

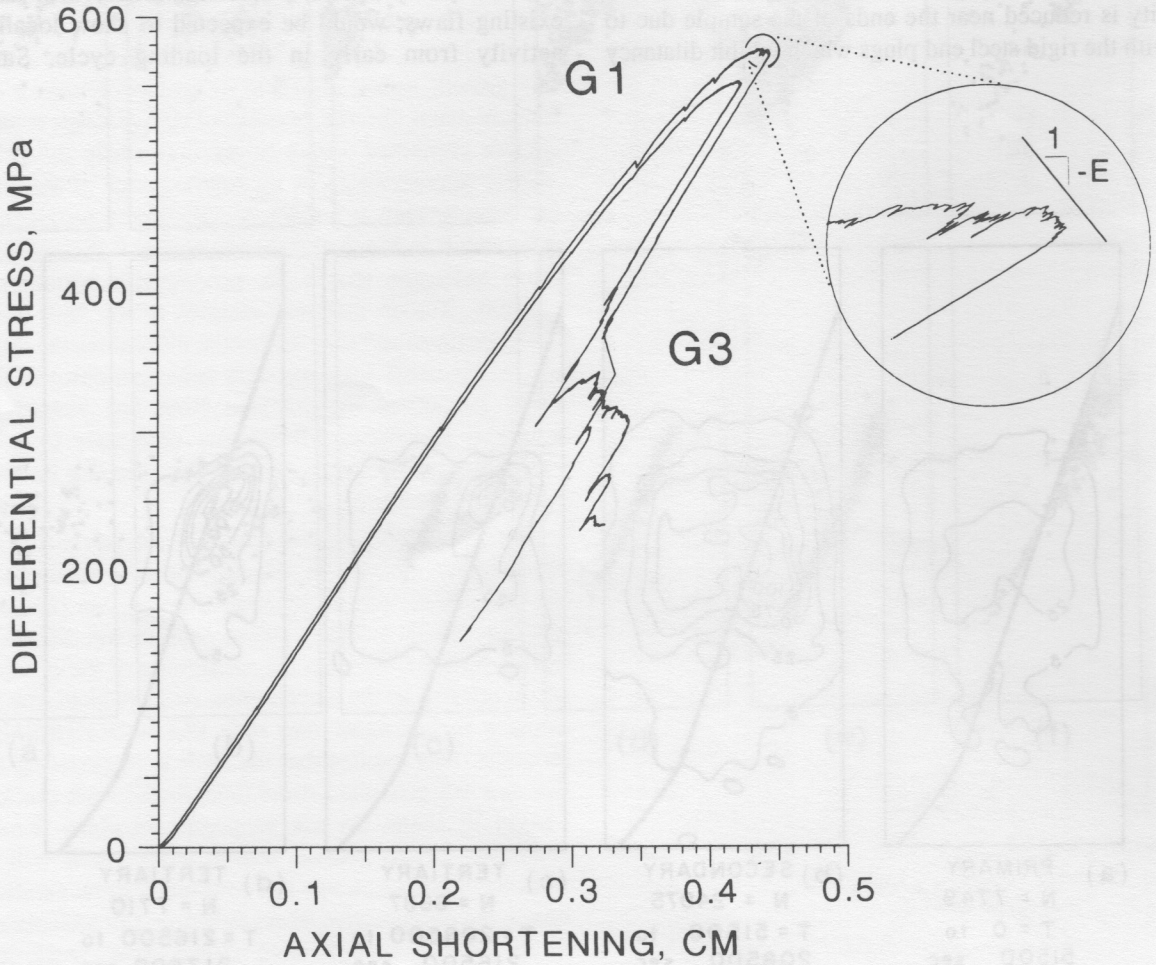

FIG 3. Differential stress/axial displacement plots for Westerly granite samples deformed at P_c = 50 MPa and constant AE rate. Fault nucleated at reversal in slope near peak stress. Loading system had to back off during fault propagation to suppress dynamic fault growth. Insert shows detail of peak-stress region and Young's modulus of granite (see text for discussion).

in Figs 3 and 4. In both experiments, fault nucleation occurred abruptly at the reversal in slope following peak stress in the stress/displacement plots. AE hypocentral locations are shown in Figs 5 and 6. The macroscopic fault nucleates in Figs 5c and 6d and then propagates across the sample. The nucleation zone of approximately 2 cm^3, rapidly evolves into the nascent fault, appearing as a half-penny shape that defines the position and orientation of the fracture. In all granite experiments that have been conducted, the fracture nucleates at the sample surface. Fracture is seen to propagate as a well-defined band of AE activity. This feature can be seen most clearly in Fig 7. The relative quiescence in the wake of the advancing fracture front suggests that the band of AE activity represents a process zone as modeled by *Rice* [1984].

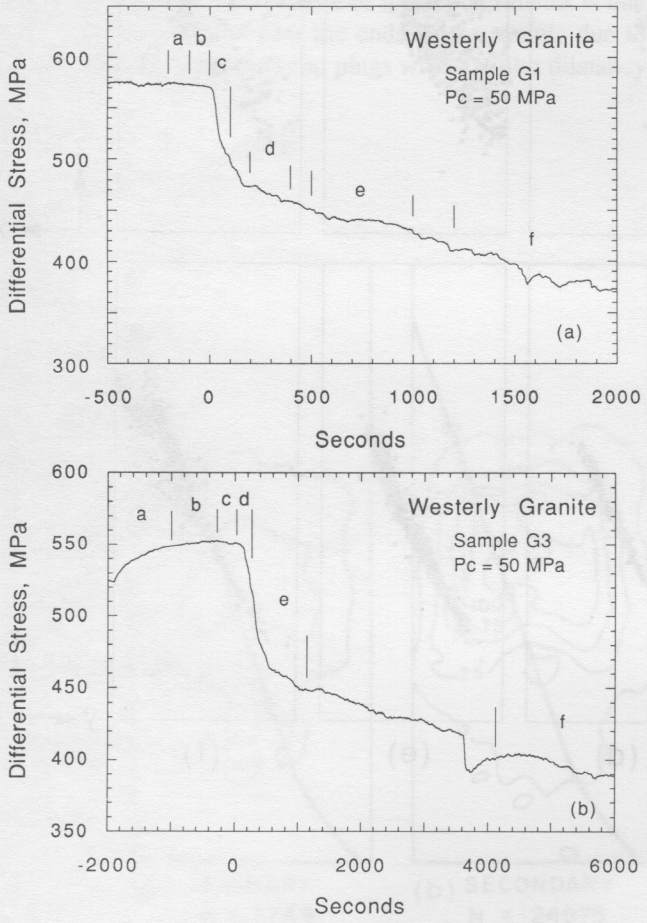

FIG 4. Stress/time plots for quasi-static faulting experiments shown in Fig 3. T = 0 was set to coincide with time of fault nucleation. Letters a - f show time intervals used to generate plots in Figs 5 and 6. Peak stress occurred at -400 s in G1 and -300 s in G3.

Bifurcation analysis of stress-sensitive dilatant material [*Rudnicki and Rice*, 1975; *Rice*, 1976; *Rudnicki*, 1977] predicts that in axisymmetric compression tests, shear localization (faulting) should occur in the post-peak-stress region. The analysis further predicts [*Rudnicki*, 1977] that the slope of the stress/strain curve should be a substantial fraction of a typical elastic modulus in magnitude at the time of localization. In the experiments shown in Figs 3 and 4, nucleation consistently occurred after peak stress, although with a weakening of less than one percent. The stress/strain slope at the time of nucleation also appears consistent with the prediction of the Rudnicki-Rice model (see insert in Fig 3).

The abruptness of the formation of the nucleation zone can be seen in Fig 7. Before nucleation, a low level of AE activity can be seen across the entire sample. This microcracking represents the diffuse background activity that would correspond to secondary creep in a creep experiment. Peak stress occurred in this period of diffuse activity at approximately 300s before nucleation. The first nucleation events occur within 0.5 cm of the sample surface and then rapidly spread inward to fill a zone about 2.6-cm-width. In a more conventional creep or constant strain rate experiment, this growth would continue to accelerate into a dynamic fracture event. Instead, because of the feedback control, fault growth continued stably at approximately 2.5 μm/s. The intense microcracking at the leading edge of the advancing fault can be seen as a ridge of AE activity progressing from right to left in Fig 7. Detailed analysis of the entire fracture front indicates that fault propagation velocity is not constant. Rather, different sections of the fault advance at different times and may reflect the difficulties the fault has in traversing small-scale strength heterogeneities in the rock. Once the advancing fracture front has passed a given position, additional AE activity continues to occur and represents crushing of grains during shearing on the newly formed fault surface.

No AE activity occurs ahead of the advancing fracture front. Subtle changes in AE patterns have been observed in the peak stress region in these experiments [*Lockner and Byerlee*, 1991]. However, these changes are diffuse and are not expected to lead to a pre-weakening of the eventual fault plane relative to the surrounding rock. Instead, the fracture appears to propagate into rock that is overall uniform in strength. This implies that the fault is propagating in-plane due to a self-generated stress field. Small-scale cracks, when loaded in shear, do not propagate in-plane [*Lawn and Wilshaw*, 1975]. Instead, tensile wing cracks will emerge from the shear crack tips and eventually grow parallel to the maximum compressive stress direction. For an isolated crack in an overall compressive stress field, work must be expended against the confining pressure to open these wing cracks. As a result, each increment of crack growth requires a corresponding increase in the remotely applied deviatoric stress. However, if a sufficiently dense population of starting flaws exists, the cracks will interact and influence each other's growth [*Reches and Lockner*, 1990]. The

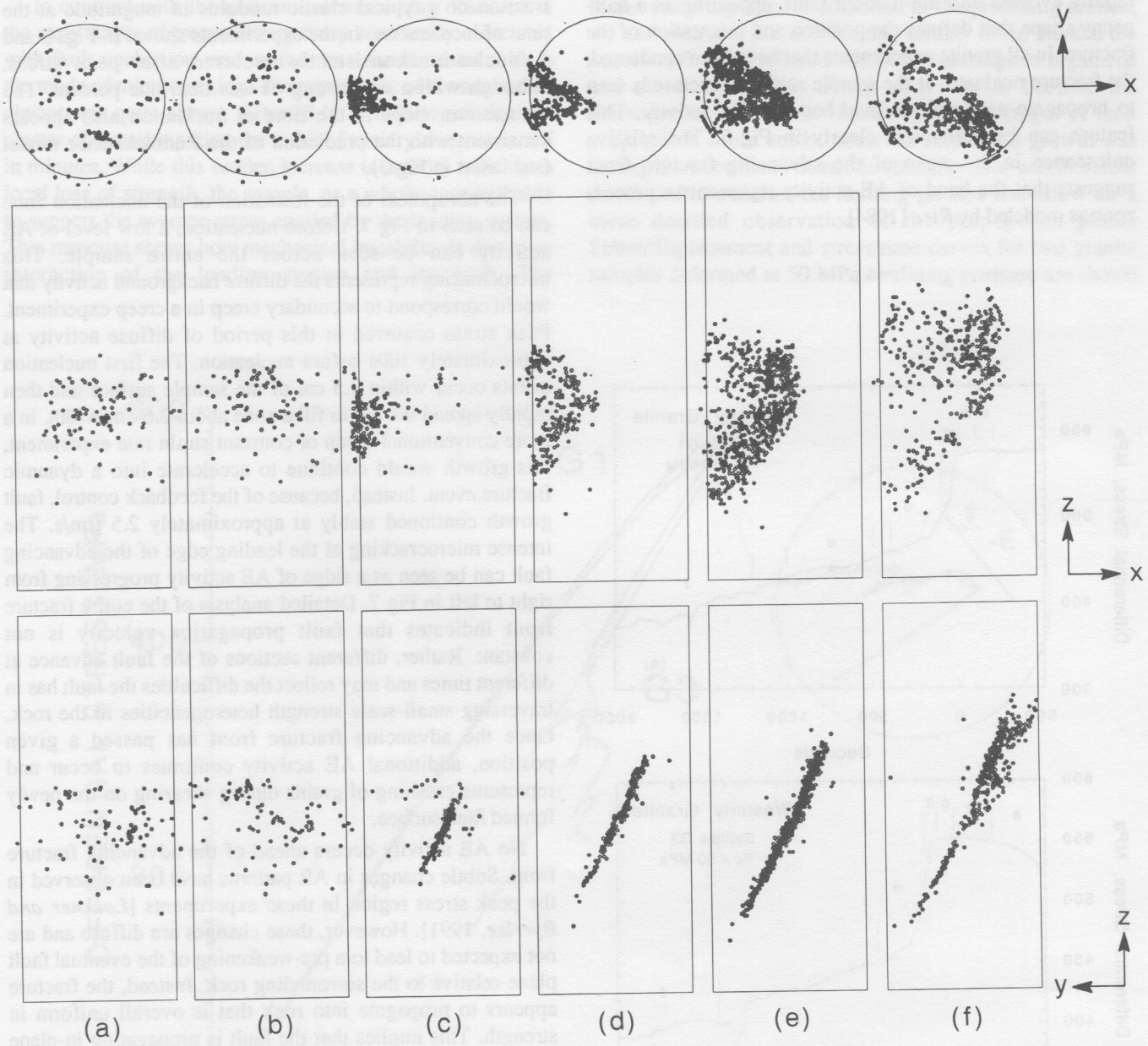

FIG 5. Macroscopic Fault Growth in Granite Sample G1 showing sequential plots of AE hypocentral locations. Time intervals used are shown in Fig 4a. a, b) pre-nucleation; c) nucleation; d - f) fault propagation. Events occurring in each time interval are shown in three projections. In the upper plots, the sample is viewed from the top. In the lower plots, the sample is viewed along-strike, so that the developing fault plane is seen as a diagonal line of AE events. The middle plots are rotated 90° and view the fault plane face-on.

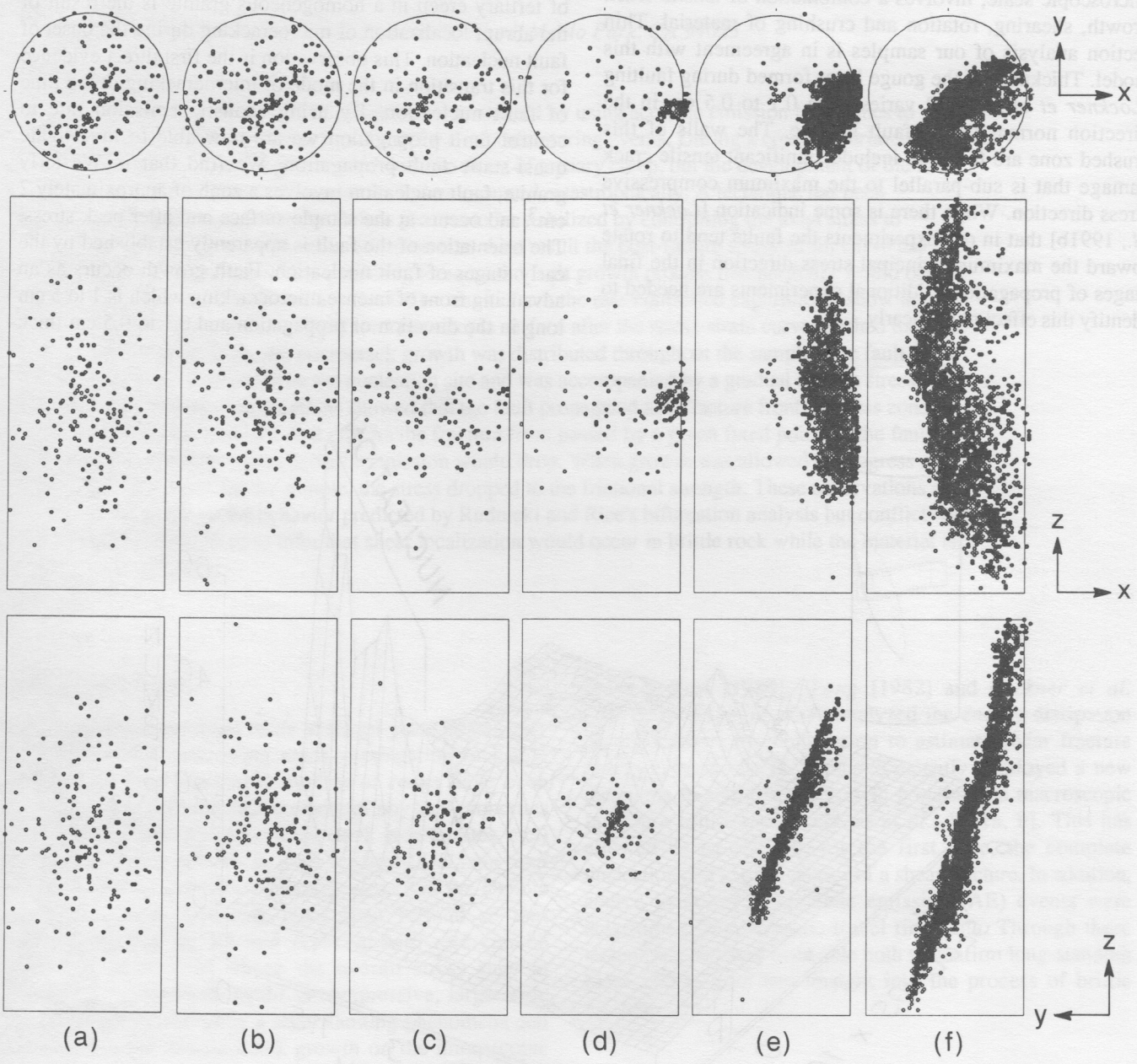

FIG 6. Macroscopic Fault Growth in Granite Sample G3 showing sequential plots of AE hypocentral locations. Time intervals used are shown in Fig 4b. a - c) pre-nucleation; d) nucleation; e, f) fault propagation. Bottom plots view sample along strike.

resulting network of open, parallel tensile cracks eventually becomes unstable and leads to rotation and crushing of microblocks to form the macroscopic fault plane. In this view of fault growth, the large-scale shear, which is able to propagate in-plane, develops a process zone that, on the microscopic scale, involves a combination of tensile crack growth, shearing, rotation and crushing of material. Thin section analysis of our samples is in agreement with this model. Thickness of the gouge layer formed during faulting [*Lockner et al.*, 1991b] varies from 0.1 to 0.5 cm in the direction normal to the fault surface. The walls of this crushed zone are found to include significant tensile crack damage that is sub-parallel to the maximum compressive stress direction. While there is some indication [*Lockner et al.*, 1991b] that in our experiments the faults tend to rotate toward the maximum principal stress direction in the final stages of propagation, additional experiments are needed to identify this effect more clearly.

CONCLUSIONS

Through the use of nondestructive acoustic emission techniques we have identified a number of important aspects of the fracture process in brittle rock. AE hypocentral locations occurring during creep demonstrate that the onset of tertiary creep in a homogeneous granite is the result of the abrupt localization of microcracking during the onset of fault nucleation. This observation is the first direct evidence for this transition in the mode of microcracking at the time of fault nucleation. By using acoustic emission rate to control fault propagation we are now able to investigate quasi-static fault propagation. We find that in Westerly granite, fault nucleation involves a zone of approximately 2 cm^3 and occurs at the sample surface and after peak stress. The orientation of the fault is apparently established by the early stages of fault nucleation. Fault growth occurs as an advancing front of intense microcracking which is 1 to 5 cm long in the direction of propagation and 0.1 to 0.5 cm thick

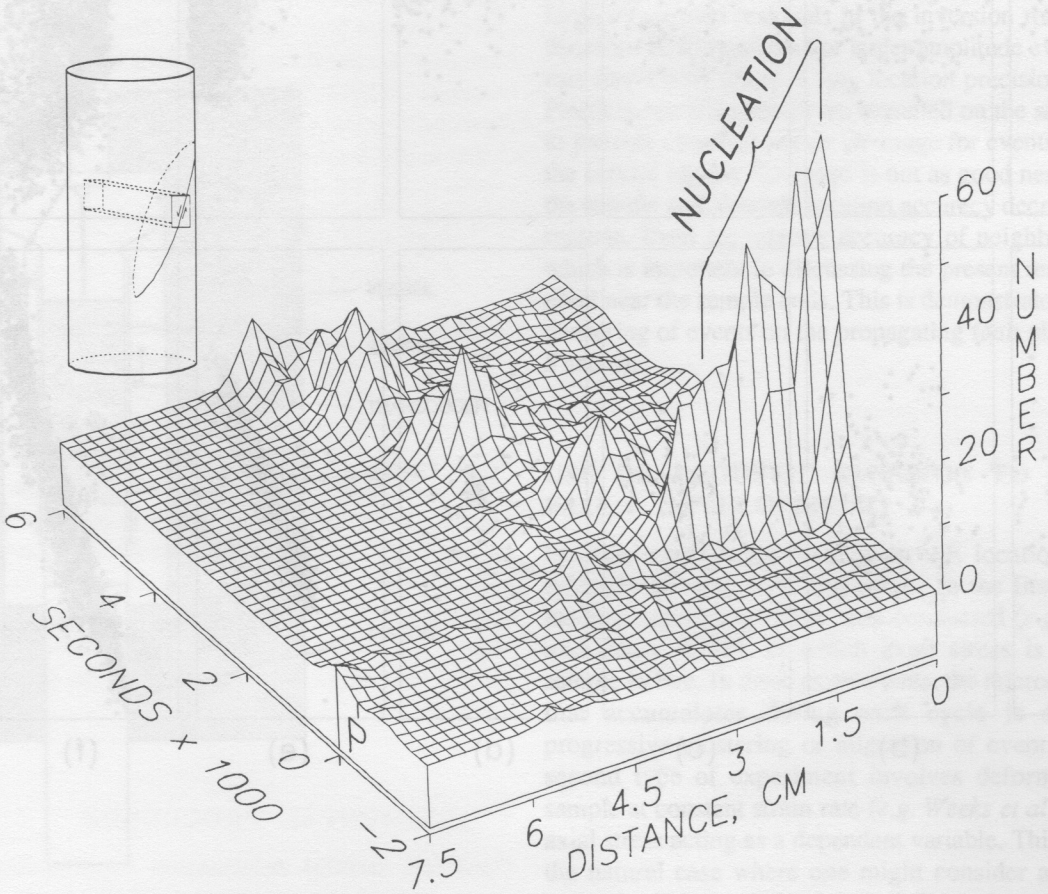

FIG 7. Fault growth in pure mode III (anti-plane) direction for experiment G3. Time axis corresponds to interval shown in Fig 4b, so that each time step represents 80 s. Distance axis is horizontal distance along fault plane from the nucleation site on the sample surface. Vertical axis is number of AE events occurring during each time step. As shown in sample diagram, events within 2 x 2 cm cross-section are included in plot. 'P' indicates time of peak stress. Fault nucleation appears as burst of AE at t = 0. Fault then propagates episodically across the sample with most activity restricted to a process zone approximately 1-cm-long in direction of propagation. No AE occurs ahead of advancing fracture front indicating that fault propagates due to a self-generated stress field.

in the direction normal to the fault. Thin section analysis shows that the gouge zone formed on the fault surface is less than 0.05 cm-thick, implying that much of the energy expended in propagation of the fracture is used to create a zone of intense microcracking along the walls of the fracture. The lack of AE in front of the advancing fault indicates that once initiated, the fault creates its own stress field which allows the fault to grow in-plane in modes II and III. Prior to nucleation, we see no significant weakening of the rock in the plane of the eventual fault. Thus these experiments provide evidence that shear fractures can propagate in plane in a homogeneous, brittle medium.

REFERENCES

Atkinson BK and Meredith PG (1987), Experimental fracture mechanics data for rocks and minerals, in *Fracture Mechanics of Rock*, BK Atkinson (ed), Academic Press, New York, 477-525.

Hirata T, Satoh T, and Ito K (1987), Fractal structure of spatial distribution of microfracturing in rock, *Geophys. J. R. Astr. Soc.* **90**, 369-374.

Lawn BR and Wilshaw TR [1975], *Fracture of Brittle Solids*, Cambridge University Press, New York, 204p.

Lockner DA and Byerlee JD (1980), Development of fracture planes during creep in granite, in *Proceedings, Second Conference on Acoustic Emission/Microseismic Activity in Geological Structures and Materials*, HR Hardy and WF Leighton (eds), Trans-Tech Publications, Clausthal-Zellerfeld, Germany, 11-25.

Lockner DA and Byerlee JD (1991), Precursory AE patterns leading to rock fracture, in *Proceedings, Fifth Conference on Acoustic Emission/Microseismic Activity in Geological Structures and Materials*, HR Hardy (ed), Trans-Tech Publications, Clausthal-Zellerfeld, Germany, 14p, in press.

Lockner DA, Byerlee JD, Kuksenko V, Ponomarev A, and Sidorin A (1991a), Quasi-static fault growth and shear fracture energy in granite, *Nature* **350**, 39-42.

Lockner DA, Byerlee JD, Kuksenko V, Ponomarev A, and Sidorin A (1991b), Observations of quasi-static fault growth from acoustic emissions, in: *Fault Mechanics and Transport Properties of Rocks*, B Evans and T-f Wong (eds), Academic Press, 34p, in press.

Nishizawa O, Onai K, and Kusunose K (1984), Hypocenter distribution and focal mechanism of AE events during two stress stage creep in Yugawara andesite, *Pure Appl. Geophys.* **122**, 36-52.

Reches Z and Lockner DA [1990], Self-organized cracking - a mechanism for brittle faulting, *EOS, Amer. Geophys. Union Trans.* **71**, 1586.

Rice JR (1976), The localization of plastic deformation, in *Proceedings of the 14th International Congress of Theoretical and Applied Mechanics* **1**, North-Holland Publishing Co., Delft, Holland, 207-220.

Rice JR (1980), The mechanics of earthquake rupture, in *Physics of the Earth's Interior*, (Proc. Int'l School of Physics "E. Fermi", course 78, 1979), AM Dziewonski and E Boschi (eds), Italian Physical Society/North Holland Publ. Co., Amsterdam, 555-649.

Rice JR (1984), Shear instability in relation to the constitutive description of fault slip, in *Proceedings, 1st Internat. Congress on Rockbursts and Seismicity in Mines, Johannesburg 1982*, SAIMM, Johannesburg, 57-62.

Rudnicki JW (1977), The effect of stress-induced anisotropy on a model of brittle rock failure as localization of deformation, in *Proceedings of the 18th U.S. Symposium on Rock Mechanics*, 8p.

Rudnicki JW and Rice JR (1975), Conditions for the localization of deformation in pressure-sensitive, dilatant materials, *J. Mech. Phys. Solids* **23**, 371-394.

Sondergeld CH and Estey LH (1981), Acoustic emission study of microfracturing during the cyclic loading of Westerly granite, *J. Geophys. Res.* **86**, 2915-2924.

Weeks JD, Lockner DA, and Byerlee JD (1978), Changes in b-value during movement on cut surfaces in granite, *Bull. of the Seismological Society of Amer.* **68**, 333-341.

Wong T-f (1982), Shear fracture energy of Westerly granite from post-failure behavior, *J. Geophys. Res.* **87**, 990-1000.

Yanagidani T, Ehara S, Nishizawa O, Kusunose K, and Terada M (1985), Localization of dilatancy in Ohshima granite under constant uniaxial stress, *J. Geophys. Res.* **90**, 6840-6858.